Wavelength-dependent Deposition of Photo-polymerized Acetylene Films

Evelyne Kasparek[1], Jason R. Tavares[2], Michael R. Wertheimer[3], Pierre-Luc Girard-Lauriault[1]

[1]*Plasma Processing Laboratory, Department of Chemical Engineering, McGill University, Montréal, Québec, Canada*
[2]*Photochemical Surface Engineering Laboratory, Department of Chemical Engineering, École Polytechnique de Montréal, Montréal, Québec, Canada*
[3]*Groupe des couches minces (GCM) and Department of Engineering Physics, École Polytechnique de Montréal, Montréal, Québec, Canada*

Abstract: Organic thin films were prepared via a photo-initiated chemical vapour deposition of acetylene (C_2H_2) using two different vacuum-ultraviolet sources, namely a Kr (λ_{peak}=123.6 nm) and a Xe (λ_{peak}=147 nm) lamp. To gain insight on growth mechanisms, film thickness, morphology and composition were studied as a function of deposition time. Both lamps yielded similar results in film composition and morphology, but differences in kinetics could be correlated to the absorption coefficients of C_2H_2 at different wavelengths.

Keywords: VUV photo-polymerization, acetylene-based thin films, film growth.

1. Introduction

Hydrocarbon-based thin films are drawing significant attention from industrial and scientific communities due to their unique and adjustable combination of properties, such as high hardness, chemical resistance, excellent tribological performance and biological properties [1, 2]. Therefore, these films show good prospects for a wide range of applications, including biomedical implants, pharmaceutical and microelectromechanical systems (MEMS) [2, 3].

Despite this great interest, the film growth mechanisms are still not fully understood [4, 5]. The main reason for this is the distribution and possible co-occurrence of different carbon hybridization states (sp^1, sp^2, sp^3), creating a large family of species (radicals, molecules and ions), all coexisting together in the gas phase. So far, these thin films have mainly been created using plasma-enhanced chemical vapour deposition (PECVD) [5]. The main initiators of chemical reactions in low-pressure plasmas are "hot" electrons, which possess a broad, Maxwell-Boltzmann-like energy distribution [6-8]. Therefore, plasmas tend to be nonselective and results are difficult to predict, adding to the difficulty in understanding the deposition mechanisms of hydrocarbon-based films.

More recently, photo-initiated CVD techniques have been used to create carbon-based films [6, 9, 10]. These techniques retain only one energy-source component of the plasma, the (UV) photons, to carry out (photo-) chemistry, thus potentially allowing for better control of the overall process.

Acetylene (C_2H_2) appears to be an ideal candidate for photo-initiated CVD due to its high reactivity and absorption coefficient over a wide range of wavelengths, as shown in Fig. 1. Additionally, polymer-like properties have been observed in the past during photolysis experiments with C_2H_2 at different wavelengths [11-13].

Danno et al. [14] created electrically resistive, optically transparent, soft amorphous carbon-hydrogen (a-C:H) thin films when irradiating acetylene using 185 nm vacuum-ultraviolet (VUV) from a low-pressure mercury lamp. Nevertheless, very few studies have been conducted aiming to understand the deposition mechanisms of these films.
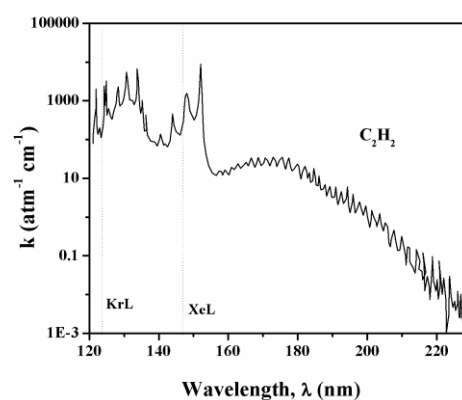

Fig. 1. UV-absorption spectrum of acetylene (adapted from [15]).

In this work, we present a wavelength-dependent study of photo-deposited acetylene-based films using two different VUV lamps. This study aims to understand the film growth mechanisms of acetylene-based films using photo-initiated CVD, since only one kind of excitation (VUV photons) at a specific wavelength will be active and available for reaction initiation.

Besides determination of the chemical composition of the coatings by X-ray photoelectron spectroscopy (XPS), deposition kinetics, the film growth and morphology, by atomic force microscopy (AFM), are also studied.

2. Experimental Methods
VUV Photo-polymerization

The reactor used for VUV photo-chemical experiments was similar to that of Truica-Marasescu et al. [6, 7, 16, 17] Briefly, it consisted of a stainless steel ''cross'' chamber, pumped down to high vacuum using a turbo-molecular pump supported by a two-stage rotary vane pump. The operating pressure during deposition was maintained near p = 15 Pa (112 mTorr). The flow rate of the hydrocarbon source gas C_2H_2 (99.6%, MEGS Inc., Montreal, QC, Canada), $F_{C_2H_2}$, was kept constant at 10 sccm using a mass flow controller (Brooks Instruments, Hatfield, PA). The polymer-like [18] coatings resulting from the photo-chemical reactions were deposited on 500 µm-thick (100) p-type silicon wafers (University Wafer, Boston, MA, USA). The frontal distance between the substrate and the two different VUV sources was adjusted so that the total photon flux, Φ, interacting with the substrate was constant, $\Phi = 5.33 \cdot 10^{14}$ ph/cm^2/s. We used non-coherent commercial VUV ("KrL" and "XeL") lamps (Resonance Ltd., Barrie, ON, Canada), based on an electrodeless radio-frequency (r.f., 100 MHz)-powered discharge plasma in krypton (Kr) or xenon (Xe) gas at low pressure: The Kr or Xe gas was contained in a Pyrex ampoule sealed with a MgF_2 window (cut-off wavelength, $\lambda = 112$ nm), as described in further detail elsewhere [7, 16, 19]; the (resonant) emission wavelengths of the lamps were $\lambda_{Kr} = 123.6$ nm (photon energy ca. 10 eV) and $\lambda_{Xe} = 147$ nm (photon energy ca. 8.4 eV). The photon energies of both lamps were sufficient to break the C≡C bond in acetylene (bond energy ca. 8.3 eV). Five different treatment durations were studied, namely, 5, 10, 15, 20 and 30 min, in order to study the effect on film thickness, composition and growth.

The experimental setup was housed inside a N_2-filled glovebox, therefore inhibiting oxygen-induced ageing of the deposited films.

X-ray Photoelectron Spectroscopy

All deposits were characterized by X-ray photoelectron spectroscopy (XPS), performed in a Thermo Scientific K-Alpha™ instrument (Waltham, MA, USA) using a monochromatic Al Kα radiation source ($hv = 1486.6$ eV). The samples were mounted onto a vacuum transfer module (VTM, Thermo Scientific K-Alpha™) inside the glovebox and directly transferred to the instrument without exposure to air, allowing determination of the films' "real" chemical composition without ageing.

The elemental composition in atomic %, (at. %) and chemical environment of the constituent elements in the deposits were obtained from XPS analyses. Survey spectra were acquired at a pass energy of 160 eV, a dwell time of 200 ms and energy steps of 1 eV, at 0° emission angles, normal to the sample surface; possible charging was corrected by referencing all peaks to the C1s peak at binding energy (BE) = 285.0 eV. The constituent elements were quantified from the broad-scan spectra using 2.3.16 PR 1.6 Casa XPS software, by integrating the areas under relevant peaks after a Shirley-type background subtraction, and by using sensitivity factors from the Wagner table.

Profilometry

The thickness of deposits was determined by profilometry, using a Dektak XT™ Stylus Profilomter (Bruker, Tucson, AZ, USA).

Atomic Force Microscopy

The morphology of deposits was investigated by atomic force microscopy (AFM) using a MFP-3D instrument (Asylum Research, Santa Barbara, CA, USA). All samples were deposited on 500 µm-thick (100) p-type silicon wafers (University Wafer, Boston, MA, USA) and measured in tapping mode using silicon cantilevers (ACTA model, AppNano) with a nominal spring constant of 37 N/m, nominal resonant frequency of 300 kHz, and nominal tip radius of 6 nm. Gwyddion 2.47 software was used to process the AFM images.

3. Results and Discussion
Deposition Kinetics and Chemical Composition

Fig. 2 shows a plot of film thickness, d, versus time, t, for acetylene-based a-C:H films deposited with KrL and XeL lamps. As expected, d increased linearly with t for both sources, thereby showing constant deposition rates, r. r was observed to be higher for the XeL lamp, roughly 7.5 nm/min compared with 5.6 nm/min for the KrL lamp.
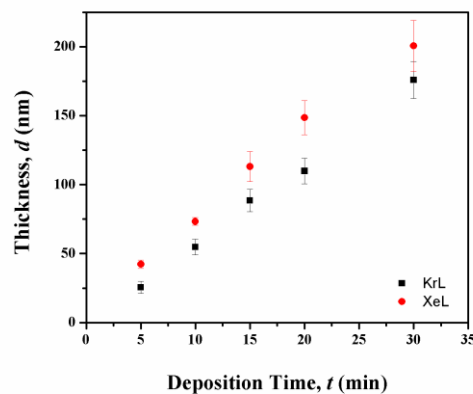

Fig. 2. Film thickness, d, as a function of deposition time, t (red circles, XeL lamp; black squares, KrL lamp).

Since the distance between the sample and the VUV sources was adjusted to assure the same photon flux, this means that d depended only on the wavelength, λ. Therefore, we can explain the higher R value for the XeL source by the higher absorption coefficient, k, of C_2H_2 at $\lambda=147$ nm compared with that at $\lambda=123.6$ nm (see Fig. 1, k(KrL)=112 atm^{-1} cm^{-2} and k(XeL)=303 atm^{-1} cm^{-2}).

Compared to the work of Danno et al. [14], where $\lambda=185$ nm was used to deposit a-C:H films, the present R values were about 7 and 9 times higher for the KrL and XeL sources, respectively. This can presumably also be

attributed to some extent to the higher k at lower wavelengths (Fig. 1), although Φ may have differed significantly.

It is noteworthy that the a-C:H films' chemical composition was substantially the same for both lamps and did not change over time, as confirmed by XPS.

Morphology and Film Growth

Fig. 3 shows AFM images for the two types of coatings at different t. These can provide insight into the a-C:H film growth modes [10, 20].
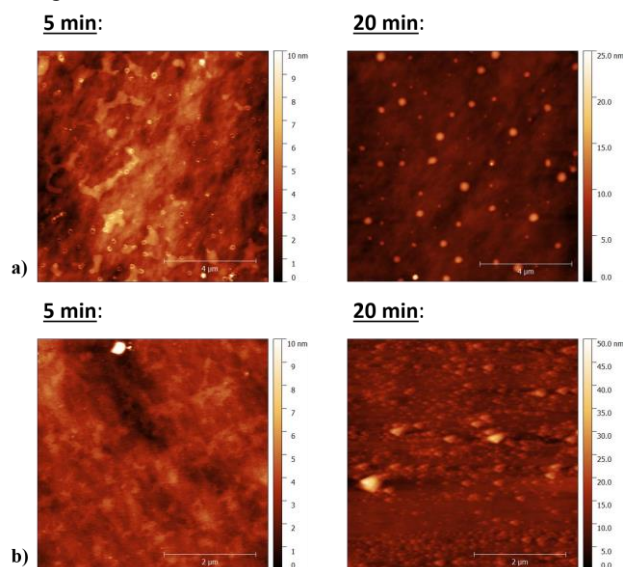

Fig. 3. AFM images of the a-C:H morphology for films deposited using the (a) KrL and (b) XeL VUV source at different deposition times, t.

Irrespective of the VUV lamp, similar a-C:H morphologies were observed, along with full coverage of the substrate after t=5 min; this was confirmed by XPS, since no Si peak from the substrate was observed. The a-C:H films were smooth from the first moments of growth, but accompanied by small round features at all values of t. After t=5 min, their height was ~2nm, then increasing further up to ~10nm. During Volmer-Weber growth, incoming precursors adhere to the surface to form clusters which can grow into 3D islands. Such islands can continue to grow but can also coalesce into a chemically homogeneous rough surface [21]. This is not observed in Fig. 3, even after t=30 min. Instead, the features were seen to grow in height, but not to coalesce, although they appear to be more abundant in the a-C:H films for the XeL source. This behaviour has been reported by Michelmore et al. [20] for the case of plasma-polymerized allylamine films. Those authors concluded that macroscopic clusters were created by oligomerization reactions in the gas phase during plasma polymerization, particles that then adhered and grew on the substrate surface [22]. Such oligomerization reactions are also feasible during VUV photolysis of acetylene and they

might well explain the present observations, but detailed analysis of the particles would help to confirm this and to better understand the growth mechanisms of the a-C:H films.

4. Conclusions

With this wavelength-dependent study, we have been able to show that a-C:H films can be obtained by photolysis of acetylene with different VUV sources, namely KrL (λ=123.6 nm) and XeL (λ=147 nm) lamps in this present research. We showed that the different photon energies influenced deposition kinetics, and that AFM-based morphologies of these a-C:H films cannot be readily explained by known growth modes. We believe that this λ-dependent VUV photolysis study can be useful in elucidating film growth activated by a single, well-characterized source of energy, unlike the case of PECVD, for example. So far, we have found that R correlated well with k, but in ongoing work the VUV wavelength will be extended upward to λ=172 nm and 185 nm.

5. Acknowledgment

6. References

[1] R. Hauert, Diamond and Related Materials, **12**, 3 (2003).
[2] C. A. K. Charitidis, E. P.; Dragatogiannis, D. A., Lubricants, **1** (2013).
[3] C. A. Charitidis, International Journal of Refractory Metals & Hard Materials, **28** (2010).
[4] J. Benedikt, Journal of Physics D-Applied Physics, **43** (2010).
[5] A. Hamdan, G. Al Makdessi, and J. Margot, Thin Solid Films, **599** (2016).
[6] F. Truica-Marasescu, J. C. Ruiz, and M. R. Wertheimer, Plasma Processes and Polymers, **9** (2012).
[7] F. Truica-Marasescu and M. R. Wertheimer, Macromolecular Chemistry and Physics, **209** (2008).
[8] J. C. Ruiz, P. L. Girard-Lauriault, and M. R. Wertheimer, Plasma Processes and Polymers, **12** (2015).
[9] C. A. Dorval Dion and J. R. Tavares, Powder Technology, **239**, 5 (2013).
[10] D. Farhanian, G. De Crescenzo, and J. R. Tavares, Langmuir, **33** (2017).
[11] H. Okabe, *Photochemistry of small molecules*. New York: Wiley, 1978.
[12] H. Okabe, Journal of Chemical Physics, **75**, (1981).
[13] L. J. Stief, V. J. Decarlo, and R. J. Mataloni, Journal of Chemical Physics, **42** (1965).
[14] M. Danno and M. Hanabusa, Materials Letters, **4** (1986).

[15] C. Y. R. Wu, F. Z. Chen, and D. L. Judge, Journal of Geophysical Research-Planets, **106**, (2001).

[16] F. Truica-Marasescu and M. R. Wertheimer, Journal of Applied Polymer Science, **91** (2004).

[17] J. C. Ruiz, A. St-Georges-Robillard, C. Theresy, S. Lerouge, and M. R. Wertheimer, Plasma Processes and Polymers, **7** (2010).

[18] Chun Q. Yong, Jongryang Joo, and Donggeun Jung, Japanese Journal of Applied Physics, **38** (1999).

[19] F. Truica-Marasescu, S. Pham, and M. R. Wertheimer, Nuclear Instruments and Methods in Physics Research Section B: Beam Interactions with Materials and Atoms, **265**, (2007).

[20] A. Michelmore, P. Martinek, V. Sah, R. D. Short, and K. Vasilev, Plasma Processes and Polymers, **8** (2011).

[21] A. Michelmore, Thin Film Coatings for Biomaterials and Biomedical Applications, ed: Woodhead Publishing (2016).

[22] A. J. Beck, S. Candan, R. D. Short, A. Goodyear, and N. S. J. Braithwaite, Journal of Physical Chemistry B, **105** (2001).